Human CD1d knock-in mouse model demonstrates potent antitumor potential of human CD1d-restricted invariant natural killer T cells

Xiangshu Wen[a], Ping Rao[a,1], Leandro J. Carreño[b,c], Seil Kim[a], Agnieszka Lawrenczyk[a], Steven A. Porcelli[b], Peter Cresswell[d,e,2], and Weiming Yuan[a,2]

[a]Department of Molecular Microbiology and Immunology, Keck School of Medicine, University of Southern California, Los Angeles, CA 90033; [b]Department of Microbiology and Immunology, Albert Einstein College of Medicine, Yeshiva University, Bronx, NY 10461; [c]Millennium Institute on Immunology and Immunotherapy, Facultad de Medicina, Universidad de Chile, Santiago 8380453, Chile; and [d]Howard Hughes Medical Institute and [e]Department of Immunobiology, Yale University School of Medicine, New Haven, CT 06520

Contributed by Peter Cresswell, January 9, 2013 (sent for review December 4, 2012)

Despite a high degree of conservation, subtle but important differences exist between the CD1d antigen presentation pathways of humans and mice. These differences may account for the minimal success of natural killer T (NKT) cell-based antitumor therapies in human clinical trials, which contrast strongly with the powerful antitumor effects in conventional mouse models. To develop an accurate model for in vivo human CD1d (hCD1d) antigen presentation, we have generated a hCD1d knock-in (hCD1d-KI) mouse. In these mice, hCD1d is expressed in a native tissue distribution pattern and supports NKT cell development. Reduced numbers of invariant NKT (iNKT) cells were observed, but at an abundance comparable to that in most normal humans. These iNKT cells predominantly expressed mouse Vβ8, the homolog of human Vβ11, and phenotypically resembled human iNKT cells in their reduced expression of CD4. Importantly, iNKT cells in hCD1d knock-in mice exert a potent antitumor function in a melanoma challenge model. Our results show that replacement of mCD1d by hCD1d can select a population of functional iNKT cells closely resembling human iNKT cells. These hCD1d knock-in mice will allow more accurate in vivo modeling of human iNKT cell responses and will facilitate the preclinical assessment of iNKT cell-targeted antitumor therapies.

humanized mouse | immunotherapy | antitumor immunity

Type 1 or invariant natural killer T (iNKT) cells are among the first responders during many types of immune responses and play critical immunomodulatory functions in diverse immunologic, infectious, and neoplastic diseases (1). The key molecule involved in the thymic selection, development, and immune recognition by iNKT cells is CD1d, a nonpolymorphic MHC I-like surface glycoprotein (1). The human CD1d (hCD1d) and mouse CD1d (mCD1d) proteins are largely conserved in amino acid sequence and 3D structure (1, 2). However, many subtle but important differences exist between hCD1d and mCD1d, including differences in their affinities for various lipid ligands and iNKT cell T cell receptors (TCRs) (2, 3), as well as clearly delineated differences in 3D structures (4) and intracellular trafficking properties (5, 6). On the other hand, iNKT cells in the human and mouse have several notable differences, particularly in their relative abundance among lymphocyte subpopulations (7) and their expression of phenotypic markers (1, 8).

Evidence for iNKT cell functions in antitumor immunity initially came from studies in mice of the potent antitumor activity of α-galactosylceramide (α-GalCer), a marine sponge-derived glycolipid that activates most iNKT cells (9). Extensive studies from many groups have substantiated this protective role of iNKT cells against tumors in mice (10, 11). Several phase-I exploratory trials of the anticancer activity of α-GalCer in humans have been reported (reviewed in ref. 12), but these have not shown consistent therapeutic benefit. The sharp discrepancy between the results obtained in tumor-bearing mice and human cancer patients treated with α-GalCer may be related to the differences between human and mouse CD1d molecules, and related differences in CD1d-restricted iNKT cells. In particular, the much greater abundance of iNKT cells in mice compared with humans has been considered to be a major flaw with conventional mouse models, limiting their predictive utility for humans. However, data for in vivo human CD1d lipid presentation are sparse and originate from a very limited number of human patients. To establish a small animal model for in vivo study of human CD1d presentation of lipids to NKT cells, we report an hCD1d knock-in (hCD1d-KI) mouse that provides a unique model that more accurately replicates features of iNKT cell responses in humans.

Results and Discussion

Generation of hCD1d Knock-in Mice and Their hCD1d Expression in Vivo. In previously reported hCD1d transgenic models, the expression of hCD1d is either restricted to thymocytes or dendritic cells (13) or widely expressed in all nucleated cells (14). To mimic the natural CD1d expression pattern, we generated mice in which hCD1d was expressed under control of the endogenous mCD1d promoter and regulatory elements. The promoter regions of hCD1D and mCD1D genes have homologous sequences containing putative binding sites for at least some transcriptional factors (15, 16). However, to ensure the compatibility with mouse transcriptional factors and proper temporal and spatial expression of hCD1d in the mouse, we generated a gene targeting construct in which a human genomic fragment containing all six exons of the human CD1D gene was fused to mouse genomic fragments flanking the mouse CD1D1 coding region (Fig. 1*A*). In mice, there are two CD1D genes, designated CD1D1 and CD1D2 (1). Whereas CD1D1 has been found to play the major role in NKT cell development and function, the function of CD1D2 is unclear, but it is expressed at the cell surface of thymocytes in some mouse strains including CD1D1-deficient mice derived from 129 embryonic stem (ES) cells used in most gene targeting (17). However, CD1D2 is a pseudogene in the C57BL/6 strain (18). We therefore used ES cells of this strain for gene targeting to replace mouse CD1D1 with the human CD1D sequence (Fig. 1*A*). This ensured that hCD1d is the only restricting molecule for NKT development and function in the resulting animals.

Author contributions: X.W., P.R., S.A.P., P.C., and W.Y. designed research; X.W., P.R., S.K., A.L., and W.Y. performed research; X.W., P.R., L.J.C., S.K., S.A.P., P.C., and W.Y. analyzed data; and X.W., L.J.C., S.A.P., P.C., and W.Y. wrote the paper.

The authors declare no conflict of interest.

Freely available online through the PNAS open access option.

[1]Present address: UCLA Immunogenetics Center and Department of Pathology, University of California, Los Angeles, CA 90095.

[2]To whom correspondence may be addressed. E-mail: weiming.yuan@usc.edu or peter.cresswell@yale.edu.

This article contains supporting information online at www.pnas.org/lookup/suppl/doi:10.1073/pnas.1300200110/-/DCSupplemental.

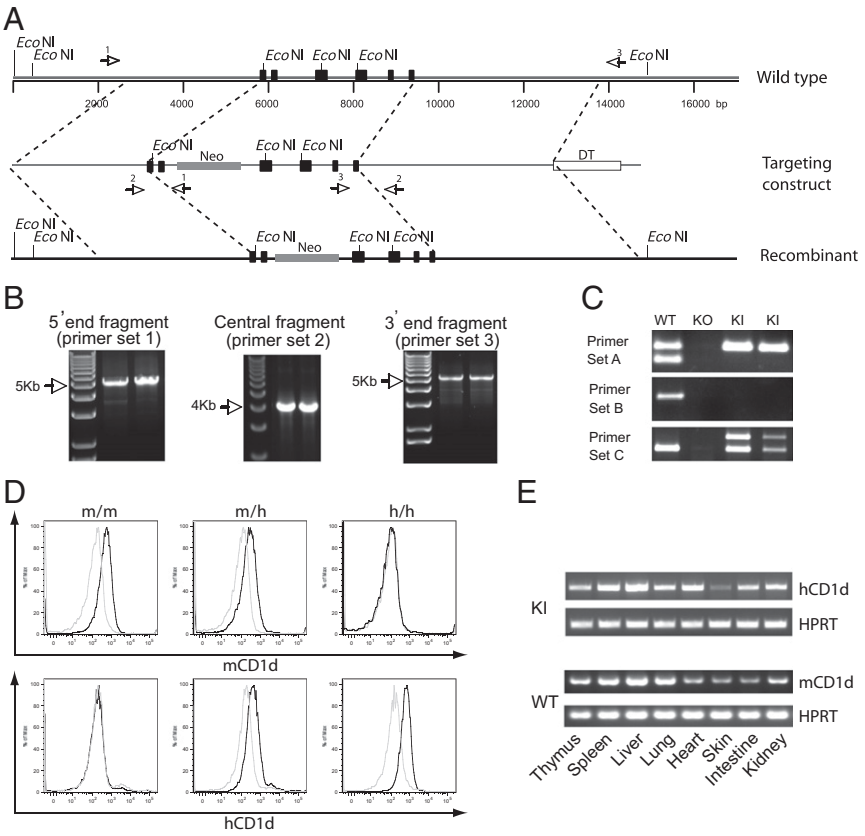

Fig. 1. Generation of an hCD1d knock-in mouse. (*A*) The physical map of mouse CD1D1 gene region before (*Top*) or after (*Bottom*) homologous recombination with the targeting construct containing hCD1d genomic sequence (*Middle*). Exons of CD1D genes are in closed boxes. Neomycin resistance gene (gray box) is inserted in the fourth intron and the diphtheria toxin (DT) gene (open box) is outside the genomic region. The three pairs of primers (1–3) used in long-range PCR of ES cell DNA are in open arrows. (*B*) DNA fragments amplified from two ES cell clones were shown. (*C*) Genotyping PCRs of two individual KI mice, WT and CD1d$^{-/-}$ mice. (*D*) Surface expression of hCD1d and mCD1d proteins in thymocytes analyzed by flow cytometry. (*E*) RT-PCR of mouse tissues with hCD1d- and mCD1d-specific primers.

The precise homologous recombination and integration of the human genomic CD1D gene in the mouse CD1D1 locus was verified by long-range PCR (Fig. 1*B*). The entire genomic region encompassing the 5′ and 3′ flanking mouse genomic fragments and the human CD1D gene was sequenced, excluding undesired mutation or recombination events. Mosaic mice with germ-line transmission of the ES cell-derived human CD1D gene were crossed to C57BL/6 mice and then intercrossed to obtain homologous KI mice. Human and mouse CD1D-specific primers were used to genotype the KI mice (Fig. 1*C*). To confirm the hCD1d protein expression, thymocytes from WT C57BL/6, heterozygous and homozygous KI mice were subjected to flow cytometry using mCD1d- and hCD1d-specific monoclonal antibodies. As expected, only hCD1d was expressed in homozygous KI mice, whereas expression of both hCD1d and mCD1d proteins could be detected in the heterozygotes at lower levels (Fig. 1*D*). To survey the tissue expression of hCD1d, we performed RT-PCR with hCD1D-specific primers. Expression of human CD1D transcripts was detected at varying levels in all tissues examined, consistent with the widespread transcription within hematopoietic lineages and low-level expression that has been reported in several types of epithelia (1). Notably, this expression pattern was similar to that of endogenous mCD1D transcripts in WT mice (Fig. 1*E*).

Efficient Presentation of Lipid Ligands by hCD1d in KI Mice. To examine the lipid-presenting function of hCD1d in the KI mice, we assayed the ability of bone marrow-derived dendritic cells (BMDCs) derived from KI mice to stimulate in vitro responses of mouse iNKT cell hybridomas to the well-characterized synthetic glycolipid α-GalCer. As expected, hCD1d expression was detected on the surface of BMDCs from hCD1d-KI but not from WT mice (Fig. 2*A*). Presentation of α-GalCer by BMDCs from KI mice was potent and generated responses of similar magnitude compared with presentation by WT BMDCs. The specificity of the responses was confirmed by blocking with species-specific mAbs reactive with mCD1d or hCD1d (Fig. 2*B*). We also observed that freshly harvested thymocytes from hCD1d-KI mice presented α-GalCer to iNKT cell hybridomas in an hCD1d-specific fashion (Fig. S1*A*), suggesting hCD1d molecules can present endogenous lipids for iNKT cell development in the KI mice.

One prominent difference that has been documented between human and mouse CD1d proteins is in their patterns of intracellular trafficking and localization. This is believed to be mainly due to a much stronger interaction of mCD1d compared with hCD1d with the clathrin adaptor protein AP-3, which routes the protein into late endosomes and lysosomes (5, 6). This interaction is required for normal iNKT cell development in mice, as well as for efficient lipid presentation of complex glycolipid antigens that require enzymatic processing in the late endosomal or lysosomal compartments (6). To examine whether hCD1d can present such complex glycolipid antigens in KI mice, we performed lipid presentation with Gal(α1→2)α−GalCer, a complex glycolipid that must be processed by the lysosomal enzyme α-galactosidase A to be recognized by iNKT TCRs (19). We indeed detected efficient presentation of the complex glycolipid to iNKT cell hybridomas (Fig. 2*C Upper*). To verify that this presentation is mediated by internationalization and processing of Gal(α1→2)α-GalCer, we fixed the BMDCs by paraformaldehyde before lipid loading and presentation. Whereas the α-GalCer could still be presented, presumably through direct loading to surface hCD1d molecules (Fig. 2*C Lower*), the presentation of Gal(α1→2)α-GalCer was completely abolished (Fig. 2C *Upper*). To examine whether hCD1d in the KI mice can present glycolipids to human iNKT cells, we performed lipid presentation assay using a human CD4+ iNKT cell line, 6F5 (20), and detected efficient presentation of both α-GalCer and Gal-α-GalCer to human NKT cells (Fig. S1*B*). Together efficient and apparent endocytosis-dependent presentation of the complex glycolipid by KI BMDC suggest that hCD1d was able to traffic into late endosomal or lysosomal compartments and access the complex

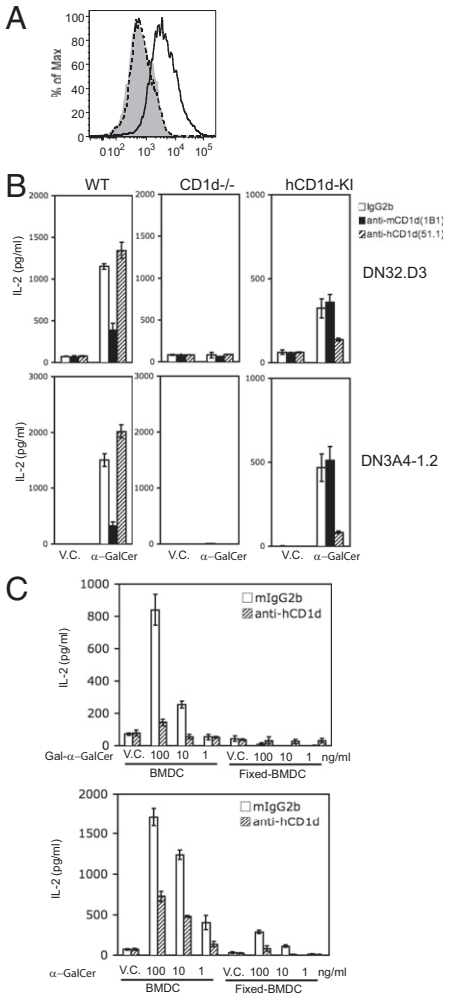

Fig. 2. Lipid presentation by hCD1d in the hCD1d-KI mouse. (*A*) hCD1d expression in BMDCs from hCD1d-KI mice (solid line) was compared with that in WT (dashed line). Isotype control is in shades. (*B*) Lipid presentation by BMDCs from WT, CD1d$^{-/-}$, and hCD1d-KI mice to mouse iNKT cell hybridoma, DN32.D3 and DN3A4-1.2. (*C*) Presentation of Gal(α-1→2)α-GalCer or α-GalCer to NKT cell hybridoma DN32.D3. Specific MAbs against hCD1d (CD1d51) or isotype control (IgG2b) were used for blocking. BMDCs were either untreated or fixed with paraformaldehyde before lipid loading. NKT cell stimulation was measured as IL-2 secretion by ELISA. V.C., vehicle control.

glycolipids, indicating a positive interaction between hCD1d and the mouse AP-3 complex.

Development of Human-Like NKT Cell Populations in hCD1d-KI Mice. Initial studies of general immune system development in hCD1d-KI mice showed no gross abnormalities in total cellularity or in lymphocyte subsets, and the mice developed and gained weight normally (Fig. S1 *C–F*). These results were consistent with earlier reports in CD1d$^{-/-}$ and hCD1d transgenic mice and indicate that ablation or alteration in CD1d expression does not significantly affect the development of conventional T, B, and dendritic cells (13, 14, 21). However, not surprisingly, we detected significant differences in NKT cell development in hCD1d-KI mice. First, there is a marked reduction in NK1.1^{+}TCRβ^{+} cells in major immune organs in the KI mice. For example, there were ∼6% of the total liver mononuclear cells in hCD1d-KI mice (Fig. 3*A Upper*), compared with ∼20% in WT mice (1). In CD1d$^{-/-}$ mice, we detected average ∼5% NK1.1^{+}TCRβ^{+} cells, which have been previously characterized as non-CD1d-restricted NKT-like T cells (22). Staining with α-GalCer loaded mCD1d tetramers showed that almost none of these NK1.1^{+}TCRβ^{+} cells were α-GalCer-reactive iNKT cells in CD1d$^{-/-}$ mice, whereas the great majority of them were tetramer-positive in WT mice. In contrast, a smaller but substantial fraction of NK1.1^{+}TCRβ^{+} cells in hCD1d-KI mice (∼27%) were tetramer-positive, most likely representing hCD1d-restricted iNKT cells (Fig. 3*B*). It is possible that a portion of the remaining 73% of NK1.1^{+}TCRβ^{+}cells are non-CD1d-restricted NKT-like cells, but some of them may also represent hCD1d-restricted noninvariant type II NKT cells. Current understanding of the TCR diversity of type II NKT cells is limited and tools to characterize the type II NKT cells are mostly restricted to sulfatide-loaded CD1d-tetramers (23, 24). Here we focused on further characterizing the type-I NKT cells of KI mice, because superior reagents are available for the study of this population.

With α-GalCer–loaded mCD1d tetramers, we clearly detected a distinct population of TCRβ^{+} tetramer^{+} iNKT cells in thymus, liver, and spleen of hCD1d-KI mice (Fig. 3*C*). Similar results were obtained with α-GalCer–loaded hCD1d tetramer (Fig. S1*G*). These cells expressed promyelocytic leukemia zinc finger, a key transcription factor directing the development of iNKT cells and other innate T cells (25) (Fig. 3*D*). These observations indicated that hCD1d efficiently presents endogenous lipid antigens to support the development of iNKT cells in the thymus, as well as maintaining in vivo homeostasis and survival of iNKT cells in periphery of hCD1d-KI mice. The abundance of iNKT cells in the thymus was ∼10% of that in WT mice (Fig. 3*C*), which is similar to what has been reported in hCD1d transgenic models (13). The much lower abundance in the thymus is most likely due to a lower iNKT cell developmental output when their thymic selection is restricted by hCD1d as opposed to mCD1d. The reason for this is not yet clear, because with the endogenous mouse CD1d promoter, the precise spatial and temporal expression and levels of hCD1d during thymic development are expected to be comparable to that of native mouse CD1d in WT mice. This suggests that an intrinsic property of the hCD1d protein is responsible for the reduced thymic output of iNKT cells in hCD1d-KI mice, which occurs similarly in humans (26). One well-documented difference between human and mouse CD1d molecules is the substantially lower affinity of hCD1d-lipid complex to NKT TCRs (2). It will be intriguing to further study how this lower affinity can potentially lead to lower NKT cell development. However, the lower abundance of iNKT cells in peripheral tissues is a function of both the thymic output of nascent iNKT cells and the homeostatic control of mature iNKT cells (1). Importantly, the abundance of iNKT cells in all tissues examined in our KI mice is comparable to that in humans, making up ∼1–2% of liver mononuclear cells and a substantially smaller fraction of splenocytes (7, 27). This indicates that our hCD1d-KI mouse will be a proper model to study the in vivo functionality of iNKT cells at an abundance similar to that found in most normal humans.

Mouse iNKT cells have limited TCR diversity, expressing an invariant TCRα chain (Vα14Jα18) paired with limited TCRβ chains (Vβ8, Vβ7, and Vβ2) (1). In hCD1d-KI mice, we detected significantly increased Vβ8 use (over 80% of all iNKT cells) in comparison with WT mice (∼50% of iNKT cells) with correspondingly lower Vβ7 use (reduced from about 13 to 7% in iNKT cells) (Fig. 3*E*). In WT mice, the remaining fraction of iNKT cells (∼35%) expresses Vβ2 and other Vβ chains, whereas in hCD1d-KI mice, this fraction accounts for only ∼9% of all iNKT cells. Vβ8 is the closest homolog to Vβ11 in human (2), the sole Vβ chain paired with the invariant TCRα chains (Vα24Jα18) in human iNKT cell TCRs (1). It is therefore reasonable to expect that Vβ8 would have greater structural compatibility with hCD1d, as suggested by the much higher affinity of hCD1d/α-GalCer complexes to mouse iNKT cell TCRs containing Vβ8 compared with those containing Vβ7 (2). This relatively high affinity may allow more efficient positive selection of Vβ8 iNKT cells during the iNKT development.

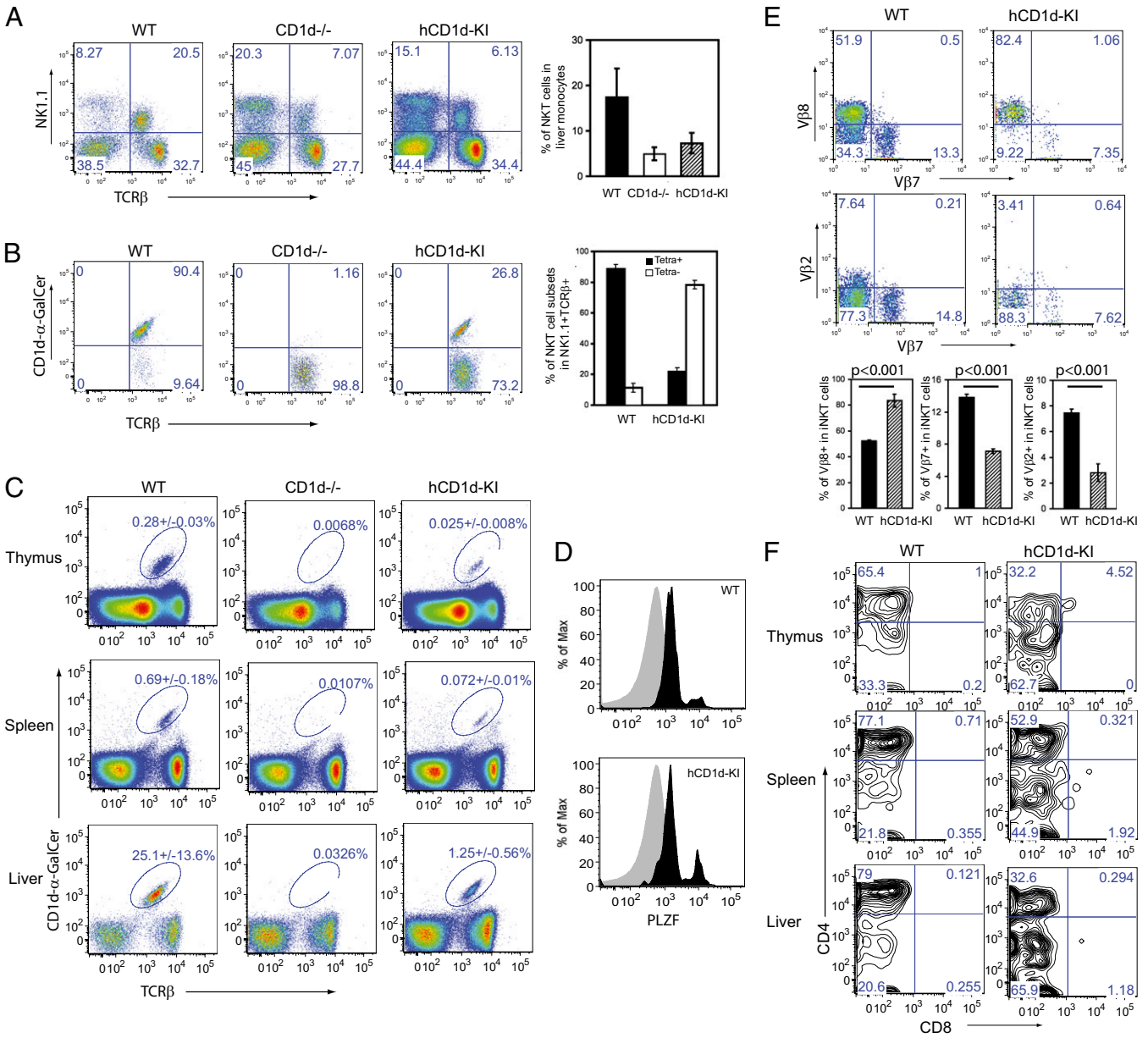

Fig. 3. Characterization of NKT cells in the hCD1d-KI mice. (*A* and *B*). Mouse liver mononuclear cells of WT, CD1d$^{-/-}$, and hCD1d-KI strains were prepared and subjected to NK1.1, TCRβ, and α-GalCer–loaded mCD1d tetramer staining. In *A*, gated NK1.1^{+} TCRβ^{+} cells were quantitated, and in *B* this population was analyzed for their tetramer staining. (*C*) Single-cell preparations from thymus, spleen, and liver monocytes in WT, CD1d$^{-/-}$, and hCD1d-KI mice were analyzed for TCRβ expression and CD1d tetramer staining. The percentage of the TCRβ^{+}CD1d-tetramer^{+} cells is presented as an average value with SD. (*D*) Gated iNKT cells from WT and hCD1d-KI mice were analyzed for promyelocytic leukemia zinc finger (PLZF) staining (black) by intracellular staining and flow cytometry. Isotype control is in gray. (*E*) Gated iNKT cells (TCRβ^{+} CD1d-tetramer^{+}) cells were analyzed for TCRβ use. (*F*) Gated iNKT cells were analyzed for CD4 and CD8 staining. All of the experiments were repeated three times for statistical analysis.

Analysis of CD4 expression by iNKT cells in hCD1d-KI mice showed a substantially lower fraction of CD4+ iNKT cells and a higher fraction with double negative (DN) phenotype in liver and spleen compared with WT mice (Fig. 3*F*). In the thymus of hCD1d-KI mice, more than half of iNKT cells were DN, also a clear increase compared with WT mice (Fig. 3*F*). Interestingly, the CD4+/DN ratio for iNKT cells in hCD1d-KI mice was similar to that reported in humans, both in peripheral blood and in the liver (7, 28). These findings suggest that hCD1d-KI mice may be useful as a model to study the development of the CD4 phenotype of human iNKT cells, and for assessing the proliferative potential of mature CD4+ versus DN iNKT cells in peripheral tissues (29).

Potent Inhibition of Tumor Metastasis by iNKT Cells in hCD1d-KI Mice. To investigate the functionality of iNKT cells in hCD1d-KI mice, we first demonstrated the presence of mRNA transcripts for IFN-γ and IL-4 in sorted peripheral CD1d tetramer+ iNKT cells (Fig. S2*A*). We then performed in vitro stimulation of iNKT cells with PMA and ionomycin and confirmed their secretion of IFN-γ and IL-4 (Fig. S2*B*). To examine the in vivo response of iNKT cells to lipid ligands, we administrated α-GalCer into the KI mice and examined cytokine secretion. Given the lower numbers of iNKT cells in hCD1d-KI mice, we expected a lower cytokine yield and therefore used a sensitive FACS-based cytokine detection assay. This demonstrated low levels of IFN-γ at 2 h, which increased at 12 h posttreatment. A detectable amount of

IL-4 was also present at 2 h posttreatment but diminished to background levels at 12 h (Fig. 4*A*). The temporal pattern of cytokine secretion was thus very similar to that observed in WT mice, although the absolute amounts of both IFN-γ and IL-4 were substantially lower (Figs. 4*A* and S2*C*).

To investigate whether iNKT cells in hCD1d-KI mice were functional in antitumor immunity, we established a B16 melanoma model in the KI mice. Congenic B16 melanoma cells were injected i.v. into KI mice, and lung metastases were enumerated 2 wk later. We administrated α-GalCer 2 d before the B16 cell injection, a well-established procedure for demonstrating antitumor function of mouse iNKT cells (30). Although a trend toward inhibition of B16 metastasis in the lung after α-GalCer administration was observed, this did not achieve statistical significance (Fig. S2*D*). To enhance the lipid presentation efficiency, we loaded autologous BMDCs from KI mice with α-GalCer and administrated these into the KI mice, a procedure reported to prolong iNKT cell responses (31). Using this approach, B16 metastasis was significantly inhibited by α-GalCer administration in hCD1d-KI mice (Fig. 4 *B*–*D*). Histologic studies showed typical metastatic B16 tumors in the lungs, with fewer metastases in the samples from α-GalCer–loaded BMDC-treated mice (Fig. 4*C*).

In summary, we have successfully generated a hCD1d-KI mouse and shown that they develop functional hCD1d-restricted iNKT cells with striking similarities to those of humans in frequency and phenotype. We also provided in vivo evidence that hCD1d can present lipids to stimulate NKT cells for anti-tumor function. Our hCD1d-KI mice thus represent a unique humanized mouse model that paves the way for further in-depth study of in vivo hCD1d lipid presentation and the identification of unique iNKT cell ligands targeting cancer and other immune diseases.

Materials and Methods

Mice. C57BL/6 mice were purchased from the Jackson Laboratory and bred locally. C57BL/6 background CD1d$^{-/-}$mice were generously provided by Chyung-Ru Wang, Northwestern University, Evanston, IL. All animal procedures were approved by the Institutional Animal Care and Use Committee at the University of Southern California.

Generation of hCD1d Knock-in Mice. The bacterial artificial chromosome clones encoding human and mouse CD1d genomic regions were obtained from BACPC Resources Center, Children's Hospital Oakland Research Institute, Oakland, CA. PCR was used to generate a construct encompassing the hCD1d genomic region flanked by the 5′ and 3′ regions of mouse CD1d1 genomic regions. The primers ATGGGGTGCCTGCTGTTTCTGCTG and CTCTCACAGTTCCTATCAGGGCGTCCTGTGA were used to amplify the hCD1D genomic fragment corresponding to human chromosome 1 nucleotide 3257291–3254243 (NCBI reference sequence NW_001838531.2). For mouse CD1D1 genomic fragments, 5′ end primers GTCCTGATATCTTGTCTTCCATTTGATCCATTTTTCATGTATGCC and AGCGCCAGAGTTCTACACAGCCCTCGGCTCC and 3′ end primers GCAGGAGAGGCAGGTGTAAGGAAGAG and AGGCTAGCCTCAGGCCTCCTTCTGTCTTACCTTCCC were used to amplify the 5′ and 3′ end of mouse genomic regions, respectively. The 5′ and 3′ end fragments have sequences corresponding to mouse chromosome 3 nucleotides 36185528–36190527 and 36179808–36182854, respectively (both in NCBI reference sequence NT_039240.8). The construct was generated in pEZFRTloxDT vector generously provided by Dominik Schenten (Yale University School of Medicine, New Haven, CT) and Klaus Rajewsky (Harvard Medical School, Boston, MA). Strain C57BL/6-derived embryonic stem cells were electroporated with linearized genomic DNA construct and embryonic stem cell clones were selected for G418 resistance and screened for human genomic DNA insertion by PCR. Sequence-specific primers were used to amplify the 5′, central, and 3′ end genomic fragments. The entire genomic mCD1d region with recombined human genomic region encoding hCD1d was sequenced. Neomycin-resistant ES clones were injected into mouse blastocysts to produce chimeric mice, and germ-line transmission of the human genomic DNA was verified by PCR analysis of tail DNA. In the gene-targeting construct, neomycin-resistance (NeoR) gene was flanked by yeast flippase recognition target sites. The founder mouse with ES cell-derived germ-line transmission of the hCD1D gene was further bred to flippase-transgenic mice to remove the NeoR gene. Further intercrossing was performed to obtain homozygous mice containing the hCD1D gene. Genotyping was done using mCD1D and hCD1D-specific primers to amplify genomic sequences from tail fragments to verify the presence of hCD1D and absence of mCD1D1 gene in the mice.

Cell Lines. The Vα14/Vβ8.2 iNKT cell hybridoma cell lines DN32.D3 and DN3A4-1.2 were kindly provided by Albert Bendelac (University of Chicago, Chicago, IL) and Mitch Kronenberg (La Jolla Institute for Allergy and Immunology, La Jolla, CA), respectively. Melanoma cell line B16 was kindly provided by Xue Huang and Si-Yi Chen (University of Southern California, Los Angeles, CA).

Flow Cytometry and Intracellular Cytokine Staining. Single-cell suspensions were prepared from thymus, spleen, and liver in FACS staining buffer (0.5% BSA, 0.09% sodium azide) and red blood cells were removed using RBC lysis buffer (BioLegend). Cells were incubated with anti-CD16/32 to block FcγRII/III, followed by staining with fluorochrome-conjugated mAbs for mouse antigens, including FITC-mCD1d (1B1), PE-mCD1d (1B1), PerCPcy5.5-TCRb (H57-597), Alexa647-TCR Vβ8.1,8.2 (KJ16-133.18), Alexa647-TCR Vβ2 (B20.6), FITC-TCR Vβ7 (TR310), eF450-NK1.1 (PK136), PEcy7-CD4 (GK1.5), APCeF780-CD8α (53-6.7), PE-mCD1d/PBS-57 tetramer or PE-hCD1d/PBS-57 tetramer (NIH Tetramer Core Facility, Emory University, Atlanta, GA), purified mouse anti-human CD1d (CD1d51), APC-CD19 (1D3), eF450-CD11c (N148), PerCPcy5.5-

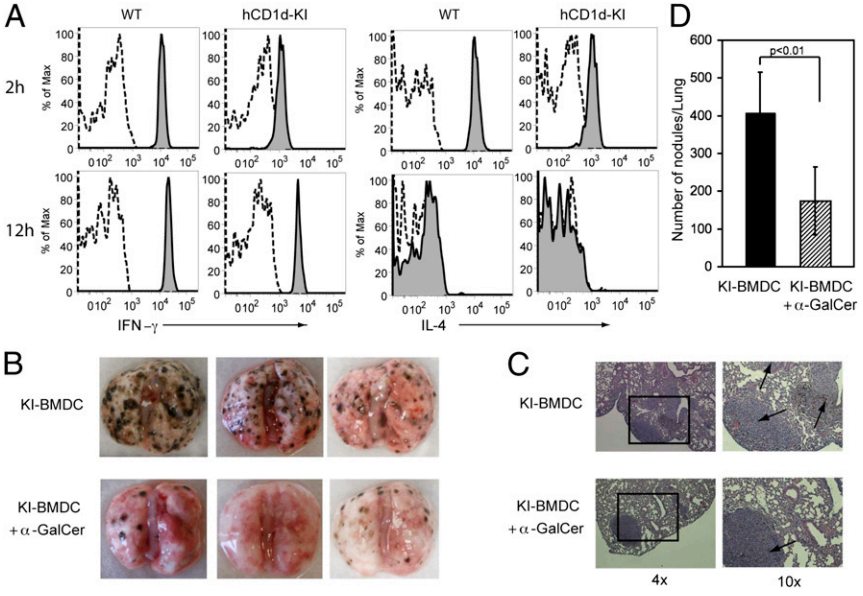

Fig. 4. Function of iNKT cells in the hCD1d-KI mice. (*A*) WT or hCD1d-KI mice were treated with vehicle control (dotted line) or α-GalCer (shaded solid line). Secretion of IFN-γ and IL-4 at 2 h and 12 h were measured by flow cytometry. (*B*) BMDCs derived from hCD1d-KI mice were unloaded or loaded with α-GalCer and i.v. injected into hCD1d-KI mice before injection of B16 melanoma cells. (*C*) Histology of representative tissues from hCD1d-KI mice treated with BMDC or BMDC loaded with α-GalCer. Metastatic tumors are indicated by arrows. (*D*) The experiments were repeated three times and lung metastases of B16 were enumerated.

IMMUNOLOGY

IFN-γ (XMG1.2), PEcy7-IL-4 (BVD6-24G2), PerCPcy5.5-Rat IgG1k isotype control (eBRG1), and PEcy7-Rat IgG1k isotype control (eBRG1). For human CD1d staining, PE-Goat anti-mouse IgG (Multiple adsorption; BD Biosciences) was used as the secondary antibody. BD Cytofix/Cytoperm Fixation/Permeabilization Solution Kit with BD GolgiPlug (BD Biosciences) was used for intracellular flow cytometry. Flow cytometry analysis was performed by FACScanto II (Becton Dickinson) and analyzed by FlowJo software.

Sorting of iNKT Cells. Spleen or liver monocytes were incubated with anti-CD90 microbeads (Miltenyi Biotec) for 20 min at 4 °C to purify T cells by AutoMACS Pro (Miltenyi Biotec). Purified T cells were used for iNKT cell sorting. The iNKT cells were sorted as $TCR\beta^+$ mCD1d/PBS-57 $tetramer^+$ cells and conventional T cells sorted as $TCR\beta^+$ mCD1d/PBS-57 $tetramer^-$ cells using a FACSAria III cell sorter (Becton Dickinson). The sorted cells were collected in complete RPMI-1640 medium and checked for their purity (>98%).

RNA Isolation, Reverse Transcription, and Quantitative RT-PCR. For RNA isolation, RNeasy Mini Kit was purchased from Qiagen and used according to the manufacturer's instructions. Reverse transcription was performed with the Transcriptor First Strand cDNA Synthesis kit (Roche). Expression of IFN-γ and IL-4 were analyzed by quantitative real-time PCR (Bio-Rad). iQ SYBR Green Supermix (Bio-Rad) was used and the reactions were performed on a CFX96 Real-Time System (Bio-Rad). PCR conditions were as follows: 95 °C for 15 min, 40 cycles at 95 °C for 15 s, 60 °C for 30 s, and 72 °C for 30 s. Target gene expression was normalized to endogenous hypoxanthine phosphoribosyltransferase level. The relative gene expression level was calculated by the $2^{-\Delta\Delta Ct}$ method.

Detection of Cytokines. For cytokine detection, mouse IFN-γ, IL-4, or IL-2 Ready-SET-Go ELISA kit (eBioscience) was performed in Immuno 96 MicroWell Solid Plates (Thermo Scientific) following the manufacturer's instructions and read by DTX880 Multimode Detector (Beckman Coulter) with multimode detection software (Beckman Coulter) under absorbance at 450 nm. For in vitro phorbol myristate acetate (PMA) and ionomycin stimulation of NKT cells, liver mononuclear cells were isolated from WT and hCD1d-KI mice and incubated with PMA (10 ng/mL) and ionomycin (1 μM) in complete medium for 5 h, with Golgiplug (500 ng/mL) present during the last 4 h. Cells were collected for cell surface staining and intracellular cytokine staining. For detection of serum cytokines, BD Cytometric Bead Array for mouse IFN-γ or IL-4 Enhanced Sensitivity Flex Set (BD Biosciences) was used following the manufacturer's instructions and analyzed by FACSCanto II (Becton Dickinson) and FCAP array software (BD Bioscience).

BMDC Preparation and Antigen Presentation Assay. BMDCs were derived using a standard method (31). Briefly, bone marrow cells were isolated from femur and tibia in complete RPMI-1640 medium, containing 10% (vol/vol) of FBS (HyClone), penicillin (50 U/mL), streptomycin (50 μg/mL), 50 ng/mL of recombinant mGM-CSF (R&D), and 25 ng/mL of recombinant mIL-4 (R&D) in RPMI-1640 (Cellgro) and cultured for 7 d in a humidified 5% (vol/vol) CO_2 incubator at 37 °C. Bacterial lipopolysaccharide (LPS; Sigma) was added at 1 μg/mL in the last 16 h for DC maturation. The resulting BMDCs (>90% $CD11c^+$) were cultured with DN32.D3 or DN3A4-1.2 in the presence or absence of α–GalCer or Gal(α-1→2)α-GalCer [100 ng/mL, generously provided by Gurdyal S. Besra (University of Birmingham, Birmingham, United Kingdom)] and Michael Brenner (Harvard Medical School, Boston, MA) and anti-mCD1d (1B1) or anti-hCD1d (CD1d51) for 24 h. For fixation of BMDC for antigen presentation, 4% (vol/vol) of paraformaldehyde was used to fix the BMDCs at room temperature for 15 min before incubating of BMDCs with lipids and NKT cell hybridomas.

In Vivo Immunization. Mice were immunized i.v. with 2 μg of α-GalCer or vehicle. Their thymus, spleen, and liver were collected at various time points after injection for analyses. For BMDC-mediated lipid delivery, on day 6 of the BMDC preparation, cells were pulsed with α-GalCer (100 ng/mL) or vehicle (0.025% of polysolvate 20) at 37 °C in a 5% (vol/vol) CO_2 incubator for 40 h, and 1 μg/mL of LPS was added for the final 16 h. After washing extensively, 1–3×10^6 nonadherent cells were i.v. injected to recipient mice as vehicle-BMDC or α-GalCer–pulsed BMDCs 1 d before the administration of B16 melanoma cells.

Determination of Melanoma Lung Metastases. The development of melanoma lung metastases was initiated by an i.v. injection with syngeneic B16 melanoma cells. After 2 wk, recipient mice were killed, their lungs were removed, and the numbers of metastatic nodules were counted under Omano OM4724 microscope in 20× magnification.

Statistical Analysis. Descriptive statistics are expressed as the mean ± SD values. Comparisons between groups were performed using two-tailed Student *t* test and a *P* value of <0.05 was considered significant.

ACKNOWLEDGMENTS. We acknowledge the technical support of the National Institutes of Health (NIH) tetramer facility at Emory University. This work was supported by NIH Grant R01 AI091987 and grants from the Harry Lloyd Charitable Trust and the Margaret Early Medical Research Trust (to W.Y.), by NIH Grant R01 AI059167 and the Howard Hughes Medical Institute (to P.C.), and by NIH Grant R01 AI45889 (to S.A.P.). L.J.C. is a Pew Latin American Fellow.

1. Brigl M, Brenner MB (2004) CD1: Antigen presentation and T cell function. *Annu Rev Immunol* 22:817–890.
2. Pellicci DG, et al. (2009) Differential recognition of CD1d-alpha-galactosyl ceramide by the V beta 8.2 and V beta 7 semi-invariant NKT T cell receptors. *Immunity* 31(1):47–59.
3. McCarthy C, et al. (2007) The length of lipids bound to human CD1d molecules modulates the affinity of NKT cell TCR and the threshold of NKT cell activation. *J Exp Med* 204(5):1131–1144.
4. Borg NA, et al. (2007) CD1d-lipid-antigen recognition by the semi-invariant NKT T-cell receptor. *Nature* 448(7149):44–49.
5. Sugita M, et al. (2002) Failure of trafficking and antigen presentation by CD1 in AP-3-deficient cells. *Immunity* 16(5):697–706.
6. Elewaut D, et al. (2003) The adaptor protein AP-3 is required for CD1d-mediated antigen presentation of glycosphingolipids and development of Valpha14i NKT cells. *J Exp Med* 198(8):1133–1146.
7. Kita H, et al. (2002) Quantitation and phenotypic analysis of natural killer T cells in primary biliary cirrhosis using a human CD1d tetramer. *Gastroenterology* 123(4):1031–1043.
8. Im JS, et al. (2008) Alteration of the relative levels of iNKT cell subsets is associated with chronic mycobacterial infections. *Clin Immunol* 127(2):214–224.
9. Kawano T, et al. (1997) CD1d-restricted and TCR-mediated activation of valpha14 NKT cells by glycosylceramides. *Science* 278(5343):1626–1629.
10. Hayakawa Y, Rovero S, Forni G, Smyth MJ (2003) Alpha-galactosylceramide (KRN7000) suppression of chemical- and oncogene-dependent carcinogenesis. *Proc Natl Acad Sci USA* 100(16):9464–9469.
11. Crowe NY, Smyth MJ, Godfrey DI (2002) A critical role for natural killer T cells in immunosurveillance of methylcholanthrene-induced sarcomas. *J Exp Med* 196(1):119–127.
12. Exley MA, Nakayama T (2011) NKT-cell-based immunotherapies in clinical trials. *Clin Immunol* 140(2):117–118.
13. Schümann J, et al. (2005) Targeted expression of human CD1d in transgenic mice reveals independent roles for thymocytes and thymic APCs in positive and negative selection of Valpha14i NKT cells. *J Immunol* 175(11):7303–7310.
14. Wang B, et al. (2001) Human CD1d functions as a transplantation antigen and a restriction element in mice. *J Immunol* 166(6):3829–3836.
15. Geng Y, Laslo P, Barton K, Wang CR (2005) Transcriptional regulation of CD1D1 by Ets family transcription factors. *J Immunol* 175(2):1022–1029.
16. Chen QY, Jackson N (2004) Human CD1D gene has TATA boxless dual promoters: An SP1-binding element determines the function of the proximal promoter. *J Immunol* 172(9):5512–5521.
17. Chen YH, et al. (1999) Expression of CD1d2 on thymocytes is not sufficient for the development of NK T cells in CD1d1-deficient mice. *J Immunol* 162(8):4560–4566.
18. Park SH, Roark JH, Bendelac A (1998) Tissue-specific recognition of mouse CD1 molecules. *J Immunol* 160(7):3128–3134.
19. Prigozy TI, et al. (2001) Glycolipid antigen processing for presentation by CD1d molecules. *Science* 291(5504):664–667.
20. Im JS, et al. (2009) Kinetics and cellular site of glycolipid loading control the outcome of natural killer T cell activation. *Immunity* 30(6):888–898.
21. Chen YH, Chiu NM, Mandal M, Wang N, Wang CR (1997) Impaired NK1+ T cell development and early IL-4 production in CD1-deficient mice. *Immunity* 6(4):459–467.
22. Matsuda JL, et al. (2000) Tracking the response of natural killer T cells to a glycolipid antigen using CD1d tetramers. *J Exp Med* 192(5):741–754.
23. Jahng AW, et al. (2001) Activation of natural killer T cells potentiates or prevents experimental autoimmune encephalomyelitis. *J Exp Med* 194(12):1789–1799.
24. Godfrey DI, Stankovic S, Baxter AG (2010) Raising the NKT cell family. *Nat Immunol* 11(3):197–206.
25. Kovalovsky D, et al. (2008) The BTB-zinc finger transcriptional regulator PLZF controls the development of invariant natural killer T cell effector functions. *Nat Immunol* 9(9):1055–1064.
26. Berzins SP, Cochrane AD, Pellicci DG, Smyth MJ, Godfrey DI (2005) Limited correlation between human thymus and blood NKT cell content revealed by an ontogeny study of paired tissue samples. *Eur J Immunol* 35(5):1399–1407.
27. Karadimitris A, et al. (2001) Human CD1d-glycolipid tetramers generated by in vitro oxidative refolding chromatography. *Proc Natl Acad Sci USA* 98(6):3294–3298.
28. Gumperz JE, Miyake S, Yamamura T, Brenner MB (2002) Functionally distinct subsets of CD1d-restricted natural killer T cells revealed by CD1d tetramer staining. *J Exp Med* 195(5):625–636.
29. Baev DV, et al. (2004) Distinct homeostatic requirements of CD4+ and CD4- subsets of Valpha24-invariant natural killer T cells in humans. *Blood* 104(13):4150–4156.
30. Schmieg J, Yang G, Franck RW, Tsuji M (2003) Superior protection against malaria and melanoma metastases by a C-glycoside analogue of the natural killer T cell ligand alpha-Galactosylceramide. *J Exp Med* 198(11):1631–1641.
31. Fujii S, Shimizu K, Kronenberg M, Steinman RM (2002) Prolonged IFN-gamma-producing NKT response induced with alpha-galactosylceramide-loaded DCs. *Nat Immunol* 3(9):867–874.